

Natural Quark Mass Patterns

K. Wang

Dept. of Physics, University of California, Los Angeles
Los Angeles, California 90024

Abstract

We incorporate the idea of natural mass matrices into the construction of phenomenologically viable quark mass matrix patterns. The general texture pattern for natural Hermitian mass matrices is obtained and several applications of this result are made.

UCLA/96/TEP/14
April 1996

Recently, we proposed the idea of natural mass matrices [1], an organizing principle useful in the construction of phenomenologically viable grand unification theory (GUT) scale quark mass matrix patterns. In this note, we present a detailed implementation and discuss certain applications of this result, among which is the construction of some supersymmetric (SUSY) GUT mass matrix patterns. We begin with a brief summary of the low energy data (LED) which we use as inputs and a discussion of the evolution of these parameters in the minimal supersymmetric standard model (MSSM). This is followed by the introduction of a convenient parametrization of Hermitian mass matrices which, along with the “naturalness” requirement [1], allows us to derive the general texture pattern for natural Hermitian quark mass matrices. The usefulness of this result is then demonstrated through several examples. Specifically, using the expression for this general pattern, we conduct an efficient viability check on a known quark mass pattern, perform an exercise of finding mass patterns with most texture-zeros and finally, we construct some simple, generic mass patterns which may be useful as templates for contemplating “predictive” quark mass Ansätze.

1. LED Inputs and Their Evolution in MSSM

In our bottom-up approach of constructing quark mass matrices, we use as inputs the quark mass ratios evaluated at $m_t \simeq 175$ (GeV) and values of CKM matrix elements in the standard Wolfenstein parametrization ¹:

Quark mass ratios	$m_u/m_t = \xi_{ut}\lambda^7$ $\xi_{ut} = 0.49 \pm 0.15$ $m_c/m_t = \xi_{ct}\lambda^4$ $\xi_{ct} = 1.46 \pm 0.13$ $m_d/m_b = \xi_{db}\lambda^4$ $\xi_{db} = 0.58 \pm 0.18$ $m_s/m_b = \xi_{sb}\lambda^2$ $\xi_{sb} = 0.55 \pm 0.18$
CKM parameters	$V_{us} = \lambda + O(\lambda^7)$ $\lambda = 0.221 \pm 0.002$ $V_{cb} = A\lambda^2 + O(\lambda^4)$ $A = 0.78 \pm 0.05$ $V_{ub} = A\sigma\lambda^3 e^{-i\delta}$ $\sigma = 0.36 \pm 0.09, \delta \simeq [45^0, 158^0]$

Table 1: LED inputs used in quark mass pattern construction.

¹See Ref. [1] for the sources of the numbers summarized in Table 1.

Notice, in particular, the different degrees of experimental uncertainties associated with the LED. Roughly speaking, $\Delta\lambda$ is about 1%, $\Delta A, \Delta\xi_{ct}$ are slightly below $O(10\%)$ while $\Delta\sigma, \Delta\xi_{ut}, \Delta\xi_{db}, \Delta\xi_{sb}$ are of $O(30\%)$ and, δ is only loosely bounded.

Additionally, one can impose the existing constraints on the relative sizes of the light quark masses from current algebra analyses [2]

$$\left(\frac{m_u}{m_d}\right)^2 + \frac{1}{Q^2}\left(\frac{m_s}{m_d}\right)^2 = 1, \quad \text{with } Q = 24 \pm 1.6. \quad (1)$$

According to a recent study [3], the value of Q in the above equation is likely to be somewhat smaller ($Q = 22.7 \pm 0.8$); and, the range of values for the quark mass ratios may be even further narrowed down to: $m_u/m_d = 0.553 \pm 0.043$ and $m_s/m_d = 18.9 \pm 0.8$. In terms of the mass ratio parameter ξ 's of Table 1, the latter translates to

$$\xi_{db}/\xi_{sb} = 1.09 \pm 0.04. \quad (2)$$

Typically, one wishes to construct mass patterns at some high energy scales as, for instance, one does when building certain GUT models. To do so using the LED inputs of Table 1, one must also take into account the evolution of these parameters. Here, as an example, we consider the scaling behavior of the LED parameters in the MSSM which actually has a rather simple description, provided that the underlying mass matrices are ‘‘natural’’ [1].² Denoting the [3,3] matrix elements of the u-type and d-type Yukawa matrices as λ_u and λ_d respectively, one has³

$$\xi_{ct}(m_G)/\xi_{ct} \simeq \xi_{ut}(m_G)/\xi_{ut} \simeq r_u, \quad (3)$$

$$\xi_{sb}(m_G)/\xi_{sb} \simeq \xi_{db}(m_G)/\xi_{db} \simeq r_d, \quad (4)$$

$$\lambda(m_G)/\lambda \simeq \sigma(m_G)/\sigma \simeq 1, \quad (5)$$

$$A(m_G)/A \simeq r \quad (6)$$

²Assuming quark and lepton mass matrices are ‘‘natural’’, the corresponding Yukawa matrices then exhibit a certain definite hierarchy. In particular, the [3,3] matrix elements are much greater than the rest – a fact gainfully exploited in the simplification of solutions to the one-loop renormalization group equations (RGE's) for the Yukawa matrices [4].

³For conciseness, unless otherwise specified, values of the parameters in the expressions below are taken to be those evaluated at m_t .

where the scaling parameters are defined by

$$\begin{aligned}
r_u &= e^{-\frac{1}{16\pi^2} \int_{\ln m_t}^{\ln m_G} \{3\lambda_u^2(\mu) + \lambda_d^2(\mu)\} d\ln \mu} , \\
r_d &= e^{-\frac{1}{16\pi^2} \int_{\ln m_t}^{\ln m_G} \{\lambda_u^2(\mu) + 3\lambda_d^2(\mu)\} d\ln \mu} , \\
r &= e^{-\frac{1}{16\pi^2} \int_{\ln m_t}^{\ln m_G} \{\lambda_u^2(\mu) + \lambda_d^2(\mu)\} d\ln \mu} .
\end{aligned} \tag{7}$$

The $\lambda(\mu)$'s in these expressions are furthermore determined from the RGE's

$$\begin{aligned}
\frac{d\lambda_u}{d\ln \mu} &\simeq \frac{1}{(4\pi)^2} \{6\lambda_u^2 + \lambda_d^2 - c_i g_i^2\} \lambda_u , \\
\frac{d\lambda_d}{d\ln \mu} &\simeq \frac{1}{(4\pi)^2} \{6\lambda_d^2 + \lambda_u^2 + \lambda_e^2 - c'_i g_i^2\} \lambda_d , \\
\frac{d\lambda_e}{d\ln \mu} &\simeq \frac{1}{(4\pi)^2} \{4\lambda_e^2 + 3\lambda_d^2 - c''_i g_i^2\} \lambda_e , \\
\frac{dg_i}{d\ln \mu} &\simeq \frac{1}{(4\pi)^2} b_i g_i^3 \quad (i = 1, 2, 3) .
\end{aligned} \tag{8}$$

Here, λ_e denotes the [3,3] matrix element of the lepton Yukawa matrix and, $c_i = (13/15, 3, 16/3)$, $c'_i = (7/15, 3, 16/3)$, $c''_i = (9/5, 3, 0)$, $b_i = (33/5, 1, -3)$. The scale $m_G \simeq 10^{16}$ (GeV) is the unification point of the three gauge couplings which we shall take to be $\alpha_i = (0.017, 0.033, 0.100)$ (with $\alpha_i \equiv g_i^2/4\pi$) following Ref. [5].

Further simplification is possible if one assumes that $\tan \beta \ll O(m_t/m_b)$, in which case the contributions of the λ_d and λ_e terms in Eq. (7) can be largely neglected and as a result, $r_d \simeq r$ and $r_u \simeq r^3$. In the same limit, the evolution of λ_u and λ_d is given by

$$\begin{aligned}
\lambda_u(\mu)/\lambda_u &\simeq \{\eta(\mu)\}^{1/2} \{1 - (3/4\pi^2) \lambda_u^2 I(\mu)\}^{-1/2} , \\
\lambda_d(\mu)/\lambda_d &\simeq \{\eta'(\mu)\}^{1/2} \{\lambda_u(\mu)/\lambda_u\}^{1/6} \{\eta(\mu)\}^{-1/12}
\end{aligned}$$

where

$$\eta(\mu) \equiv \prod_i^i \{\alpha_i/\alpha_i(\mu)\}^{c_i/b_i} , \quad \eta'(\mu) \equiv \prod_i \{\alpha_i/\alpha_i(\mu)\}^{c'_i/b_i} ,$$

and

$$I(\mu) \equiv \int_{\ln m_t}^{\ln \mu} \eta(\mu) d\ln \mu .$$

Expressed in terms of the above parameters and functions, one has

$$r \simeq \{\lambda_u(m_G)/\lambda_u\}^{-1/6} \{\eta(m_G)\}^{1/12} . \quad (9)$$

From these results one sees that $r \simeq O(1)$ except when λ_u approaches a small region defined by $\lambda_u \simeq 2\pi/\sqrt{3I(m_G)}$ where r rapidly drops to zero.

For large $\tan \beta$'s, the analysis becomes more involved and one has to rely upon numerical methods for solving Eq. (8) and evaluating the r 's in Eq. (7). Interestingly, the values of the r 's do not deviate much from being of $O(1)$ unless $\tan \beta$ reaches near the value of m_t/m_b where they begin to drastically decrease again. For a qualitative understanding of this observation, we solve Eq. (8) with the assumption $\lambda_u = \lambda_d$ (corresponding to $\tan \beta = m_t/m_b$) while momentarily ignoring contributions from the leptonic sector. In this limit, we find

$$\lambda_u(\mu) \simeq \lambda_d(\mu) \propto \{1 - (3.5/4\pi^2)I(\mu)\}^{-1/2}$$

which yields approximately $\lambda_u(m_G), \lambda_d(m_G) \rightarrow \infty$. Referring moreover to the results in Eqs. (7) and (9), we have then $r_u \simeq r_d \simeq r^2$ with $r \rightarrow 0$.

For easy reference, we include in Fig. 1 a plot based on numerical solutions of Eqs. (7) and (8) subject to the boundary condition (at m_t)⁴

$$m_t = \frac{v}{\sqrt{2}}\lambda_u \sin \beta , \quad m_b = \frac{v}{\sqrt{2}}\lambda_d \cos \beta , \quad m_\tau = \frac{v}{\sqrt{2}}\lambda_e \cos \beta$$

with $v \simeq 246.2$ (GeV), $m_t \simeq 175$ (GeV), $m_b \simeq 2.78$ (GeV) and $m_\tau \simeq 1.76$ (GeV)⁵.

2. The General Texture Pattern of Natural Hermitian Quark Mass Matrices

(i) *A Parametrization of Hermitian Quark Mass Matrices*

⁴More detailed results of some related calculations based on two-loop RGE's can be found in Ref. [6].

⁵Notice the end regions of the plot below depend rather sensitively on the exact values of the numbers taken.

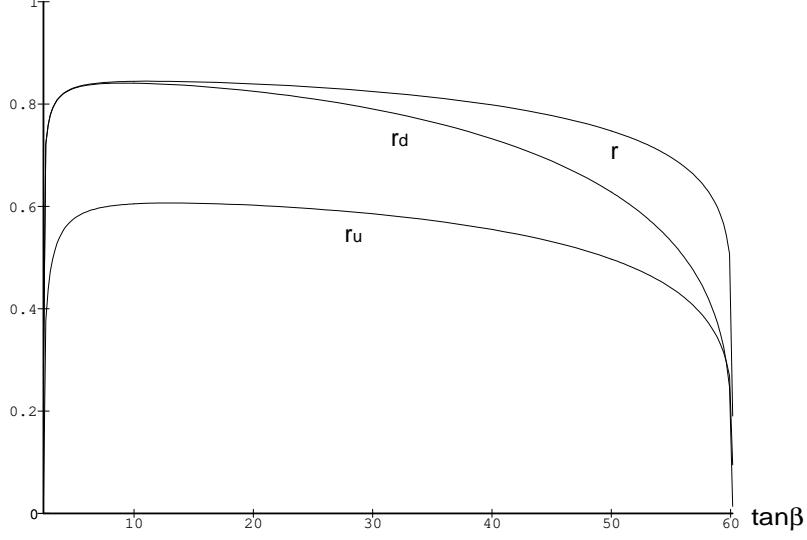


Figure 1: Scaling parameters as functions of $\tan\beta$

Given the (scaled) diagonal quark mass matrices [1]

$$\tilde{M}_u^{diag}(m_t) = \begin{pmatrix} \xi_{ut}\lambda^7 & 0 & 0 \\ 0 & \xi_{ct}\lambda^4 & 0 \\ 0 & 0 & 1 \end{pmatrix}, \quad \tilde{M}_d^{diag}(m_t) = \begin{pmatrix} \xi_{db}\lambda^4 & 0 & 0 \\ 0 & \xi_{sb}\lambda^2 & 0 \\ 0 & 0 & 1 \end{pmatrix} \quad (10)$$

and the CKM matrix (in the standard form) [7]

$$V = \begin{pmatrix} c_1c_3 & s_1c_3 & s_3e^{-i\delta} \\ -s_1c_2 - c_1s_2s_3e^{i\delta} & c_1c_2 - s_1s_2s_3e^{i\delta} & s_2c_3 \\ s_1s_2 - c_1c_2s_3e^{i\delta} & -c_1s_2 - s_1c_2s_3e^{i\delta} & c_2c_3 \end{pmatrix}, \quad (11)$$

the most general Hermitian mass matrices can be constructed from

$$\tilde{M}_u = U \tilde{M}_u^{diag} U^\dagger, \quad (12)$$

$$\tilde{M}_d = D \tilde{M}_d^{diag} D^\dagger \quad (13)$$

in which the unitary matrices U , D are subject to the constraint

$$U^\dagger D = \Phi_u V \Phi_d \quad (14)$$

where $\Phi_{u,d}$ are some diagonal phase matrices. Furthermore, aside from a trivial quark-phase redefinition (which amounts to $U \leftrightarrow \Psi U$ and $D \leftrightarrow \Psi D$,

(Ψ being some common phase matrix), one can always, for example, choose to parametrize the unitary matrices U, D according to:

$$(i) \quad D \rightarrow D_s \quad \text{and then} \quad U^\dagger \rightarrow V\Phi D_s \quad (15)$$

or somewhat analogously,

$$(ii) \quad U^\dagger \rightarrow U_s^\dagger \quad \text{and then} \quad D \rightarrow U_s\Phi'V \quad (16)$$

where D_s, U_s^\dagger are the matrices D, U^\dagger written in the standard form (of V) after necessary rephasing, and Φ, Φ' are some diagonal phase matrices which can be arranged to have only two phases in each.

In what follows, we shall adopt prescription (ii) since we have found it to be more convenient for constructing natural mass matrices⁶. Specifically, we let

$$\Phi' \equiv \begin{pmatrix} e^{i\phi} & 0 & 0 \\ 0 & e^{i\psi} & 0 \\ 0 & 0 & 1 \end{pmatrix} \quad (17)$$

and write, in terms of some orthogonal rotation matrices (C 's) and some diagonal phase matrices (Δ 's)⁷

$$V = C_2 \Delta C_3 \Delta^\dagger C_1$$

and accordingly

$$U = C_{1u} \Delta_u C_{3u} \Delta_u^\dagger C_{2u} .$$

Defining three more orthogonal matrices $C_{id} \equiv C_{iu} C_i$ ($i = 1, 2, 3$) we have, by Eq. (16),

$$D = \{C_{1d}\} \{C_1^\dagger (\Delta_u C_{3d} \Delta_u^\dagger) C_1\} \\ \{C_1^\dagger (\Delta_u C_3^\dagger \Delta_u^\dagger) (C_{2d} C_2^\dagger \Phi' C_2) (\Delta C_3 \Delta^\dagger) C_1\} .$$

(ii) *The Texture Pattern of Natural Mass Matrices*

⁶Previously, in Ref. [1], we followed (i) to construct several mass pattern examples.

⁷See Ref. [1] for the precise definitions of the matrices introduced below.

Following the procedure described in Ref. [1], we proceed to express V in the Wolfenstein parametrization [8] and likewise the matrices C 's as perturbative expansions in terms of the small parameter λ (Table 1). Subsequently, we apply our ‘‘naturalness’’ criterion [1] on the resulting quark mass matrices to arrange for natural mass patterns. Below we summarize our main result.

In terms of the CKM matrix parameters (λ , A , $\Lambda \equiv \sigma A/\lambda$, δ), the quark mass ratios (ξ 's) and the free phases (ϕ , ψ) introduced in Eq. (17), natural Hermitian quark mass matrices exhibit the following general texture pattern

$$\begin{aligned}\tilde{M}_u &= \begin{pmatrix} u_{11}\lambda^7 & u_{12}\lambda^6 & u_{13}\lambda^4 \\ u_{12}^*\lambda^6 & u_{22}\lambda^4 & u_{23}\lambda^2 \\ u_{13}^*\lambda^4 & u_{23}^*\lambda^2 & u_{33} \end{pmatrix} \\ \tilde{M}_d &= \begin{pmatrix} d_{11}\lambda^4 & d_{12}\lambda^3 & d_{13}\lambda^4 \\ d_{12}^*\lambda^3 & d_{22}\lambda^2 & d_{23}\lambda^2 \\ d_{13}^*\lambda^4 & d_{23}^*\lambda^2 & d_{33} \end{pmatrix}\end{aligned}\quad (18)$$

with, ⁸

$$\begin{aligned}u_{11} &= \xi_{ut} + \{\alpha^2\xi_{ct} + |u_{13}|^2\}\lambda + O(\lambda^2) \ , \\ u_{12} &= \alpha\xi_{ct} + u_{13}u_{23} + O(\lambda^2) \ , \\ u_{22} &= \xi_{ct} + |u_{23}|^2 + O(\lambda^2) \ , \\ u_{33} &= 1 + O(\lambda^4) \ ; \\ d_{11} &= \xi_{db} + |d_{12}|^2/\xi_{sb} + O(\lambda^2) \ , \\ d_{12} &= \xi_{sb}\{e^{i(\phi-\psi)} + \alpha\lambda\} + O(\lambda^2) \ , \\ d_{13} &= u_{13} + \alpha Ae^{i\psi} + \Lambda e^{i(\phi-\delta)} - d_{12}d_{23}\lambda + O(\lambda^2) \ , \\ d_{22} &= \xi_{sb} + O(\lambda^2) \ , \\ d_{23} &= u_{23} + Ae^{i\psi} + O(\lambda^2) \ , \\ d_{33} &= 1 + O(\lambda^4) \ .\end{aligned}\quad (19)$$

The remaining matrix element parameters in Eq. (18) are not fixed, but are constrained by our requirement of ‘‘naturalness’’ to:

$$|u_{13}|, |u_{23}|, \alpha \lesssim O(1) \ .\quad (20)$$

⁸In specifying the values of quark masses or mass ratios we conventionally quote these numbers as being positive. In the expressions below and throughout the presentation of our results however, quark masses m_q 's (and in general quark mass ratios ξ 's as well) can be chosen to have either positive or negative signs, depending upon the context of expressions they are in.

The quark mass matrices of Eq. (18), although defined apparently at the scale of m_t , can nonetheless be implemented at any energy scale so long as one properly takes into account the renormalization group (RG) evolution of the quark mass ratios and the CKM parameters in Eq. (19).

3. Applications

(i) Mass Pattern Viability Check

Given any natural mass pattern, once written in the form of Eq. (18), one can examine its viability using Eqs. (19) and (20). Specifically, the matrix elements of the pattern must, to a good approximation, obey the following constraints:

$$\begin{aligned}
& u_{22} - |u_{23}|^2 \simeq \xi_{ct} , \\
& d_{22} \simeq \xi_{sb} , \\
& |d_{23} - u_{23}| \simeq A , \\
& |d_{12}/\xi_{sb} - (u_{12} - u_{13}u_{23})\lambda/\xi_{ct}| \simeq 1 , \\
& |d_{13} - u_{13} - (d_{23} - u_{23})(u_{12} - u_{13}u_{23})/\xi_{ct} + d_{12}d_{23}\lambda| \simeq \Lambda , \\
& u_{11} - |u_{13}|^2\lambda - (|u_{12} - u_{13}u_{23}|^2/\xi_{ct})\lambda - \xi_{ut} \simeq 0 , \\
& d_{11} - (\xi_{db} + |d_{12}|^2/\xi_{sb}) \simeq 0 , \\
& \arg\{d_{13} - u_{13} - (d_{23} - u_{23})(u_{12} - u_{13}u_{23})/\xi_{ct} + d_{12}d_{23}\lambda\} \\
& - \arg\{d_{12}/\xi_{sb} - (u_{12} - u_{13}u_{23})\lambda/\xi_{ct}\} - \arg\{d_{23} - u_{23}\} \simeq -\delta . \quad (21)
\end{aligned}$$

As an illustrative example, we apply the results of Eq. (21) to the study of a mass pattern recently proposed based on the idea of a ‘‘democratic’’ symmetry [9]. In this model, after some straightforward manipulations, the quark mass matrices take the form

$$M_u \simeq m_t \begin{pmatrix} 0 & u & 0 \\ u & \frac{2}{9}\epsilon_u & -\frac{\sqrt{2}}{9}\epsilon_u \\ 0 & -\frac{\sqrt{2}}{9}\epsilon_u & 1 \end{pmatrix} , \quad M_d \simeq m_b \begin{pmatrix} 0 & de^{i\omega} & 0 \\ de^{-i\omega} & \frac{2}{9}\epsilon_d & -\frac{\sqrt{2}}{9}\epsilon_d \\ 0 & -\frac{\sqrt{2}}{9}\epsilon_d & 1 \end{pmatrix}$$

where the symmetry breaking parameters $u \ll \epsilon_u \ll 1$ and $d \ll \epsilon_d \ll 1$ are to be determined from the known values of quark masses. Using the expressions of Eq. (21), one finds $\epsilon_u \simeq (9/2)\xi_{ct}\lambda^4$, $\epsilon_d \simeq (9/2)\xi_{sb}\lambda^2$, $u \simeq \sqrt{\xi_{ut}\xi_{ct}}\lambda^{11/2}$, $d \simeq$

$\sqrt{\xi_{db}\xi_{sb}}\lambda^3$ and furthermore the following relations which can be regarded as the CKM “predictions” of the pattern:

$$\begin{aligned}\lambda &\simeq \sqrt{m_d/m_s} \pm \cos\omega\sqrt{m_u/m_c}, \\ A\lambda^2 &\simeq (m_s/m_b - m_c/m_t)/\sqrt{2}, \\ \sigma A\lambda^3 &\simeq (m_s/m_b - m_c/m_t)\sqrt{m_u/2m_c}\end{aligned}$$

and $\delta \simeq \omega + O(\lambda)$. One sees, when referring to the data in Table 1, that this pattern leads to extremely low values for $|V_{cb}|$ and $|V_{ub}|$, although it has an acceptable value for the quantity $|V_{ub}/V_{cb}|$.

(ii) *Mass Patterns with Most Texture-zeros*

Starting with Eqs. (18–20), arranging for patterns with multiple texture-zeros can be particularly efficient. As an exercise, we insert zeros in all possible entries of the mass matrices of Eq. (18). We find, in this way, a total of five allowable five-texture-zero, low energy (at the scale of m_t) patterns. To ensure consistence with the LED, the matrix elements of these five-texture-zero patterns are specified in accordance with Eq. (19). In Table 2 we list these patterns and their CKM constraints or “predictions”⁹.

Numerically, with the signs of the quark masses and those of the Δ terms in Table 2 judiciously chosen, the CKM predictions of these patterns can be estimated using the quark mass ratios and the value of $|V_{cb}|$ given in Table 1. As an example, in Table 4 we give some results, corresponding to a certain possible choice of the aforementioned signs. In addition we have also included estimates with the much more stringent constraint of Eq. (2) taken into account.

To implement the above five-texture-zeros patterns at the GUT scale in the MSSM, the only necessary modification required of Tables 2 and 3 is the insertion of the RG scaling factors (r_u 's, r_d 's and r 's) in front of the quark mass ratios and the parameters V_{cb} and V_{ub} , based on Eqs. (3–6). Having done so, one sees that the CKM predictions of patterns 1, 2 and

⁹“Predictions” ensue whenever certain matrix elements or parameters are overspecified [1]. For each of the mass patterns in Table 2, for example, Eq. (19) renders two of the LED parameters dependent (chosen here to be λ and Λ or, equivalently, $|V_{us}|$ and $|V_{ub}|$) while the remaining ones are not overspecified and as a result, their experimental values can always be accomodated.

	\tilde{M}_u	\tilde{M}_d	“Prediction”
1	$\begin{pmatrix} 0 & u_{12}\lambda^6 & 0 \\ u_{12}\lambda^6 & u_{22}\lambda^4 & 0 \\ 0 & 0 & u_{33} \end{pmatrix}$	$\begin{pmatrix} 0 & d_{12}\lambda^3 & 0 \\ d_{12}^*\lambda^3 & d_{22}\lambda^2 & d_{23}\lambda^2 \\ 0 & d_{23}\lambda^2 & d_{33} \end{pmatrix}$	$ V_{us} = \sqrt{m_d/m_s} \pm \Delta_{11} + O(\lambda^3)$ $ V_{ub} = V_{cb} \sqrt{m_u/m_c} \pm \Delta_{12} + O(\lambda^6)$
2	$\begin{pmatrix} 0 & u_{12}\lambda^6 & 0 \\ u_{12}\lambda^6 & 0 & u_{23}\lambda^2 \\ 0 & u_{23}\lambda^2 & u_{33} \end{pmatrix}$	$\begin{pmatrix} 0 & d_{12}\lambda^3 & 0 \\ d_{12}^*\lambda^3 & d_{22}\lambda^2 & d_{23}\lambda^2 \\ 0 & d_{23}^*\lambda^2 & d_{33} \end{pmatrix}$	$ V_{us} = \sqrt{m_d/m_s} \pm \Delta_{21} + O(\lambda^3)$ $ V_{ub} = V_{cb} \sqrt{m_u/m_c} \pm \Delta_{22} + O(\lambda^6)$
3	$\begin{pmatrix} 0 & 0 & u_{13}\lambda^4 \\ 0 & u_{22}\lambda^4 & 0 \\ u_{13}\lambda^4 & 0 & u_{33} \end{pmatrix}$	$\begin{pmatrix} 0 & d_{12}\lambda^3 & 0 \\ d_{12}^*\lambda^3 & d_{22}\lambda^2 & d_{23}\lambda^2 \\ 0 & d_{23}\lambda^2 & d_{33} \end{pmatrix}$	$ V_{us} = \sqrt{m_d/m_s} + \Delta_{31} + O(\lambda^3)$ $ V_{ub} = \sqrt{m_u/m_t} \pm \Delta_{32} + O(\lambda^6)$
4	$\begin{pmatrix} 0 & u_{12}\lambda^6 & 0 \\ u_{12}\lambda^6 & u_{22}\lambda^4 & u_{23}\lambda^2 \\ 0 & u_{23}\lambda^2 & u_{33} \end{pmatrix}$	$\begin{pmatrix} 0 & d_{12}\lambda^3 & 0 \\ d_{12}^*\lambda^3 & d_{22}\lambda^2 & 0 \\ 0 & 0 & d_{33} \end{pmatrix}$	$ V_{us} = \sqrt{m_d/m_s} \pm \Delta_{41} + O(\lambda^3)$ $ V_{ub} = V_{cb} \sqrt{m_u/m_c} + \Delta_{42} + O(\lambda^6)$
5	$\begin{pmatrix} 0 & 0 & u_{13}\lambda^4 \\ 0 & u_{22}\lambda^4 & u_{23}\lambda^2 \\ u_{13}\lambda^4 & u_{23}\lambda^2 & u_{33} \end{pmatrix}$	$\begin{pmatrix} 0 & d_{12}\lambda^3 & 0 \\ d_{12}^*\lambda^3 & d_{22}\lambda^2 & 0 \\ 0 & 0 & d_{33} \end{pmatrix}$	$ V_{us} = \sqrt{m_d/m_s} \pm \Delta_{51} + O(\lambda^3)$ $ V_{ub} = \sqrt{m_u/m_c} \{- V_{cb} ^2 + m_c/m_t\}^{1/2} + \Delta_{52} + O(\lambda^6)$

Table 2: Quark mass patterns with five texture-zeros and their “predictions”. (The subleading terms Δ ’s in the above expressions for $|V_{cs}|$ and $|V_{cb}|$ are relegated to Table 3.)

$\Delta_{11} = \cos \delta \sqrt{\frac{m_u}{m_c}}$	$\Delta_{12} = \cos \delta \frac{\sqrt{m_d m_s}}{m_b} V_{cb} $
$\Delta_{21} = \cos \delta \sqrt{\frac{m_u}{m_c}}$	$\Delta_{22} = \cos \delta \frac{\sqrt{m_d m_s}}{m_b} (V_{cb} + \sqrt{\frac{m_c}{m_t}}) \ddagger$
$\Delta_{31} = 0$	$\Delta_{32} = \cos \delta \frac{\sqrt{m_d m_s}}{m_b} V_{cb} $
$\Delta_{41} = \cos \delta \sqrt{\frac{m_u}{m_c}}$	$\Delta_{42} = 0$
$\Delta_{51} = \cos \delta \sqrt{\frac{m_u}{m_c}} (1 + \frac{m_s}{m_t} V_{cb} ^{-2})^{-1/2}$	$\Delta_{52} = 0$

Table 3: Expressions for the subleading terms in the last column of Table 2. (\ddagger For definiteness, we assume for this number the special case $\arg\{d_{23}\} = 0$ and also $d_{23} > 0$.)

	λ	σ
1	$(0.23 \pm 0.05) + (0.06 \pm 0.01) \cos \delta$ $\{(0.23 \pm 0.01) + (0.06 \pm 0.01) \cos \delta\}$	$(0.27 \pm 0.05) + (0.03 \pm 0.01) \cos \delta$ $\{(0.27 \pm 0.05) + (0.03 \pm 0.01) \cos \delta\}$
2	$(0.23 \pm 0.05) + (0.06 \pm 0.01) \cos \delta$ $\{(0.23 \pm 0.01) + (0.06 \pm 0.01) \cos \delta\}$	$(0.27 \pm 0.05) + (0.08 \pm 0.03) \cos \delta$ $\{(0.27 \pm 0.05) + (0.08 \pm 0.03) \cos \delta\}$
3	0.23 ± 0.05 $\{0.23 \pm 0.01\}$	$(0.42 \pm 0.07) + (0.03 \pm 0.01) \cos \delta$ $\{(0.42 \pm 0.07) + (0.03 \pm 0.01) \cos \delta\}$
4	$(0.23 \pm 0.05) + (0.06 \pm 0.01) \cos \delta$ $\{(0.23 \pm 0.01) + (0.06 \pm 0.01) \cos \delta\}$	0.27 ± 0.05 $\{0.27 \pm 0.05\}$
5	$(0.23 \pm 0.05) + (0.03 \pm 0.01) \cos \delta$ $\{(0.23 \pm 0.01) + (0.03 \pm 0.01) \cos \delta\}$	0.32 ± 0.08 $\{0.32 \pm 0.08\}$

Table 4: Numerical estimates for the CKM “predictions” of the five-texture-zero patterns. (Numbers in the curly brackets are results incorporating the additional constraint of Eq. (2).)

4 are unaltered to the leading order in λ and therefore, these patterns are also viable as SUSY GUT patterns; the same is true for patterns 3 and 5 for most values of $\tan\beta$ ¹⁰. However, near the end regions of the plot in Fig. 1 (where for example $\tan\beta$ is very small), the $|V_{ub}|$ predictions of these patterns can become unsound. Incidentally, as it was observed in Ref. [10], the nearest conceivable six-texture-zero SUSY GUT pattern corresponds to pattern 2 in Table 2 with the parameter d_{23} of \tilde{M}_d set to zero. As a result, this pattern generates an extra, but unfortunately generally unfavorable, CKM “prediction” $|V_{cb}| = \{\sqrt{r_u/r^2}\}\sqrt{m_c/m_t} + O(\lambda^4)$ (since the ratio r_u/r^2 is typically close to 1 according to Fig. 1). Nonetheless, in light of our discussion on the evolution of the LED parameters, this six-texture-zero pattern could still be viable, should the scenario in which $\tan\beta \ll O(m_t/m_b)$ (consequently $r_u/r^2 \simeq r$) and furthermore $r \simeq O(\lambda)$ prevails.

The detailed CKM “predictions” of the five patterns given here can be used to further speculate in favor of (or against) them, especially if experimental data becomes more precise. For instance, taking into account Eq. (2) one sees from Tables 3 and 4 that for patterns 1, 2 and 4 to be successful, the CP phase δ must be quite large. The same is true for pattern 5, although to a slightly lesser degree. On the other hand, pattern 3 imposes no such restriction, instead it favors a somewhat larger $|V_{ub}|$ when compared to the rest.

(iii) *Mass Patterns Useful as Templates*

By relating the matrix elements in Eq. (18) which may have similar orders of magnitude, one can search or arrange for patterns that have fewer independent parameters and thus that have potentially greater predictive power. Below, we provide five such simple quark mass patterns in Table 5 (and the CKM “predictions” of these patterns in Table 6) with the hope that they may be useful as templates for contemplating quark mass Ansätze.¹¹

In deriving the results of Tables 5 and 6, the parameters (x, y, z) ’s are assumed to be of $O(1)$ or less, but are otherwise unspecified. This allows for

¹⁰This is consistent with the findings of Ref. [10] where these five-texture-zero patterns, obtained through a detailed numerical analysis, were first presented.

¹¹To implement these patterns at the GUT scale in the MSSM, one simply takes into account the RG scaling of the quark mass ratios and the CKM parameters in Table 6, in complete analogy to the previous case of five-texture-zero patterns.

	\tilde{M}_u	\tilde{M}_d
1	$\begin{pmatrix} \lesssim O(\lambda^9) & \lesssim O(\lambda^6) & y_u B e^{-i\phi_u} \lambda^4 \\ \lesssim O(\lambda^6) & B\lambda^4 & x_u B\lambda^4 \\ y_u B e^{i\phi_u} \lambda^4 & x_u B\lambda^4 & A \end{pmatrix}$	$\begin{pmatrix} \lesssim O(\lambda^6) & F e^{-i\psi_d} \lambda^3 & y_d F e^{-i\phi_d} \lambda^3 \\ F e^{i\psi_d} \lambda^3 & E\lambda^2 & x_d E\lambda^2 \\ y_d F e^{i\phi_d} \lambda^3 & x_d E\lambda^2 & D \end{pmatrix}$
2	$\begin{pmatrix} C\lambda^7 & z_u C\lambda^7 & y_u B e^{-i\phi_u} \lambda^4 \\ z_u C\lambda^7 & B\lambda^4 & x_u B\lambda^4 \\ y_u B e^{i\phi_u} \lambda^4 & x_u B\lambda^4 & A \end{pmatrix}$	$\begin{pmatrix} \lesssim O(\lambda^6) & F e^{-i\psi_d} \lambda^3 & y_d F e^{-i\phi_d} \lambda^3 \\ F e^{i\psi_d} \lambda^3 & E\lambda^2 & x_d E\lambda^2 \\ y_d F e^{i\phi_d} \lambda^3 & x_d E\lambda^2 & D \end{pmatrix}$
3	$\begin{pmatrix} \lesssim O(\lambda^9) & C\lambda^6 & \lesssim O(\lambda^6) \\ C\lambda^6 & \lesssim O(\lambda^6) & B\lambda^2 \\ \lesssim O(\lambda^6) & B\lambda^2 & A \end{pmatrix}$	$\begin{pmatrix} \lesssim O(\lambda^6) & F e^{-i\psi_d} \lambda^3 & y_d F e^{-i\phi_d} \lambda^3 \\ F e^{i\psi_d} \lambda^3 & E\lambda^2 & x_d E\lambda^2 \\ y_d F e^{i\phi_d} \lambda^3 & x_d E\lambda^2 & D \end{pmatrix}$
4	$\begin{pmatrix} C\lambda^7 & z_u C\lambda^7 & \lesssim O(\lambda^6) \\ z_u C\lambda^7 & \lesssim O(\lambda^6) & B\lambda^2 \\ \lesssim O(\lambda^6) & B\lambda^2 & A \end{pmatrix}$	$\begin{pmatrix} \lesssim O(\lambda^6) & F e^{-i\psi_d} \lambda^3 & y_d F e^{-i\phi_d} \lambda^3 \\ F e^{i\psi_d} \lambda^3 & E\lambda^2 & x_d E\lambda^2 \\ y_d F e^{i\phi_d} \lambda^3 & x_d E\lambda^2 & D \end{pmatrix}$
5	$\begin{pmatrix} \lesssim O(\lambda^9) & \lesssim O(\lambda^8) & C\lambda^4 \\ \lesssim O(\lambda^8) & x_u C\lambda^4 & B\lambda^2 \\ C\lambda^4 & B\lambda^2 & A \end{pmatrix}$	$\begin{pmatrix} \lesssim O(\lambda^6) & F e^{-i\psi_d} \lambda^3 & y_d F e^{-i\phi_d} \lambda^3 \\ F e^{i\psi_d} \lambda^3 & E\lambda^2 & x_d E\lambda^2 \\ y_d F e^{i\phi_d} \lambda^3 & x_d E\lambda^2 & D \end{pmatrix}$

Table 5: Quark mass patterns which may be useful as templates. (In the above, $(A, B\dots F)$ are fixed parameters of $O(1)$ and (x, y, z) 's are adjustable parameters.)

certain flexibility in pattern-fitting. Evidently, not all values for the (x, y, z) 's work equally well; using Table 6 and the LED of Table 1 however, one can readily determine the feasibility of a given set of values for these adjustable parameters.

Certainly, construction of more elaborate patterns is also possible. But already, a host of interesting patterns can be obtained from Table 5. In particular, notice that texture-zeros can easily be accommodated by inserting them where allowed or by selectively specifying some of the (x, y, z) 's to be 0's.¹² Similarly, equalities among matrix elements can be arranged by specifying some of the (x, y, z) 's to be 1's. As an illustrative example, let us

¹²In fact, the five-texture-zero patterns of Table 2 can be gotten this way as well.

	$ V_{us} $	$ V_{cb} $	V_{ub}
1	$\sqrt{\frac{m_d}{m_s}}$ $\pm \cos \psi_d \sqrt{\frac{m_u}{m_c} + y_u^2 \frac{m_c}{m_t}}$ $+O(\lambda^3)$	$x_d \frac{m_s}{m_b}$ $+x_u \frac{m_c}{m_t}$ $+O(\lambda^4)$	$\left\{ y_d \frac{\sqrt{m_d m_s}}{m_b} e^{-i\phi_d} + y_u \frac{m_c}{m_t} e^{-i\phi_u} \right.$ $\left. \pm \sqrt{\frac{m_u}{m_c} + y_u^2 \frac{m_c}{m_t}} V_{cb} \right\} e^{i\psi_d}$ $+x_d \left(\frac{m_s}{m_b}\right)^2 V_{us} + O(\lambda^6)$
2	$\sqrt{\frac{m_d}{m_s}}$ $+z_u \left(\frac{m_u}{m_c} + y_u^2 \frac{m_c}{m_t}\right) \cos \psi_d$ $+O(\lambda^4)$	$x_d \frac{m_s}{m_b}$ $+x_u \frac{m_c}{m_t}$ $+O(\lambda^4)$	$\left\{ y_d \frac{\sqrt{m_d m_s}}{m_b} e^{-i\phi_d} + y_u \frac{m_c}{m_t} e^{-i\phi_u} \right.$ $\left. +z_u \left(\frac{m_u}{m_c} + y_u^2 \frac{m_c}{m_t}\right) V_{cb} \right\} e^{i\psi_d}$ $+x_d \left(\frac{m_s}{m_b}\right)^2 V_{us} + O(\lambda^6)$
3	$\sqrt{\frac{m_d}{m_s}}$ $\pm \cos \psi_d \sqrt{\frac{m_u}{m_c}}$ $+O(\lambda^3)$	$\sqrt{\frac{m_c}{m_t}}$ $-x_d \frac{m_s}{m_b}$ $+O(\lambda^4)$	$\left\{ y_d \frac{\sqrt{m_d m_s}}{m_b} e^{-i\phi_d} \right.$ $\left. \pm \sqrt{\frac{m_u}{m_c}} V_{cb} \right\} e^{i\psi_d}$ $+x_d \left(\frac{m_s}{m_b}\right)^2 V_{us} + O(\lambda^6)$
4	$\sqrt{\frac{m_d}{m_s}}$ $+z_u \frac{m_u}{m_c} \cos \psi_d$ $+O(\lambda^4)$	$\sqrt{\frac{m_c}{m_t}}$ $-x_d \frac{m_s}{m_b}$ $+O(\lambda^4)$	$\left\{ y_d \frac{\sqrt{m_d m_s}}{m_b} e^{-i\phi_d} \right.$ $\left. +z_u \frac{m_u}{m_c} V_{cb} \right\} e^{i\psi_d}$ $+x_d \left(\frac{m_s}{m_b}\right)^2 V_{us} + O(\lambda^6)$
5	$\sqrt{\frac{m_d}{m_s}}$ $+ \cos \psi_d \sqrt{\frac{m_u}{m_c} (1+w)}$ $+O(\lambda^4) \ddagger$	$\sqrt{\frac{m_c}{m_t} (1+w^{-1})}$ $-x_d \frac{m_s}{m_b}$ $+O(\lambda^4) \ddagger$	$\left\{ y_d \frac{\sqrt{m_d m_s}}{m_b} e^{-i\phi_d} - \sqrt{\frac{m_u}{m_t} w} \right.$ $\left. + \sqrt{\frac{m_u}{m_c} (1+w)} V_{cb} \right\} e^{i\psi_d}$ $+x_d \left(\frac{m_s}{m_b}\right)^2 V_{us} + O(\lambda^6) \ddagger$

Table 6: CKM ‘‘Predictions’’ of the patterns in Table 5. (‡ In these expressions, w is defined to be the quantity $\left\{ \frac{m_c^2}{x_u^2 m_u m_t} \right\}^{\frac{1}{3}}$ for notational brevity.)

choose in pattern 2, $y_d = 0$, $x_u = y_u = z_u = x_d = 1$, and $\psi_d = \pi$; the result is a rather simple looking pattern in which

$$\tilde{M}_u = \begin{pmatrix} C\lambda^7 & C\lambda^7 & B\lambda^4 e^{-i\phi_u} \\ C\lambda^7 & B\lambda^4 & B\lambda^4 \\ B\lambda^4 e^{i\phi_u} & B\lambda^4 & A \end{pmatrix}, \quad \tilde{M}_d = \begin{pmatrix} 0 & F\lambda^3 & 0 \\ F\lambda^3 & E\lambda^2 & E\lambda^2 \\ 0 & E\lambda^2 & D \end{pmatrix}.$$

As a low energy pattern, it gives, to a very good approximation, the CKM “predictions”:

$$|V_{us}| \simeq \sqrt{\frac{m_d}{m_s}} - \frac{m_u}{m_c} - \frac{m_c}{m_t}, \quad |V_{cb}| \simeq \frac{m_s}{m_b} + \frac{m_c}{m_t}, \quad |V_{ub}| \simeq \frac{m_c}{m_t}$$

and $\delta \simeq \phi_u - \pi$ (which of course yields the correct value for δ automatically when ϕ_u is suitably chosen). To check the soundness of the above “predictions”, we input the quark mass ratios of Table 1 and find

$$|V_{us}| \simeq 0.22 \pm 0.05, \quad |V_{cb}| \simeq 0.030 \pm 0.009, \quad \text{and} \quad |V_{ub}| \simeq 0.0034 \pm 0.0003$$

in reasonable agreement with the CKM data, also given in Table 1. (If we incorporate Eq. (2) into the calculation of $|V_{us}|$ above, we have instead $|V_{us}| \simeq 0.22 \pm 0.01$.) Correspondingly, as a SUSY GUT pattern, it predicts:

$$|V_{us}| \simeq \sqrt{\frac{m_d}{m_s}} - \frac{m_u}{m_c} - \{r_u\} \frac{m_c}{m_t}, \quad |V_{cb}| \simeq \left\{ \frac{r_d}{r} \right\} \frac{m_s}{m_b} + \left\{ \frac{r_u}{r} \right\} \frac{m_c}{m_t}, \quad |V_{ub}| \simeq \left\{ \frac{r_u}{r} \right\} \frac{m_c}{m_t}$$

and again $\delta \simeq \phi_u - \pi$. Since for most values of $\tan \beta$, $r_d/r \simeq 1$ and r_u/r is of $O(1)$ (Fig. 1), one sees that these GUT pattern “predictions” are equally “sound”, with possible exceptions noted for extreme values of $\tan \beta$.

It is worth pointing out that using the results of Eqs. (18–20), the quark mass patterns of our examples are constructed in a completely systematic and often very efficient manner; moreover, “predictions” of these mass patterns are readily obtained in the form of explicit analytical expressions – making transparent the viability conditions of each pattern.

Acknowledgements

I would like to thank Professor Roberto Peccei for suggesting this project and for many valuable comments. This work is supported in part by the Department of Energy under Grant No. FG03-91ER40662.

References

- [1] R. D. Peccei and K. Wang, Phys. Rev. D53 (1996) 2712
- [2] D. Kaplan and A. Manohar, Phys. Rev. Lett. 56 (1986) 2004; H. Leutwyler, Nucl. Phys. B337 (1990) 108
- [3] H. Leutwyler, CERN preprint CERN-TH/96-44
- [4] K. Sasaki, Z. Phys. C32 (1986) 149; K. S. Babu, Z. Phys. C35 (1987) 69; M. Olechowski and S. Pokorski, Phys. Lett. B257 (1991) 388
- [5] S. Dimopoulos, L. Hall and S. Raby, Phys. Rev. D45 (1992) 4192; G. Anderson, S. Raby, S. Dimopoulos, and L. J. Hall, Phys. Rev. D47 (1993) 3702
- [6] V. Barger, M. S. Berger and P. Ohmann, Phys. Rev. D47 (1993) 1093
- [7] Particle Data Group: L. Montanet *et al.*, Phys. Rev. D50 (1994) 1173
- [8] L. Wolfenstein, Phys. Rev. Lett. 51 (1983) 1945
- [9] H. Fritzsch, preprint MPI-PhT/95-02; H. Fritzsch and Z. Xing, Phys. Lett. B353 (1995) 114
- [10] P. Ramond, R.G. Roberts and G.G. Ross, Nucl. Phys. B406 (1993) 19